4th International Conference on
Earthquake Geotechnical Engineering
June 25-28, 2007
Paper No. 1190

FREE-FIELD MOTIONS IN THE INHOMOGENEOUS HALFPLANE

George MANOLIS[1], Tsviatko RANGELOV[2], Petia DINEVA[3], Christos PANAGIOTOPOULOS[4]

ABSTRACT

This work presents closed-form solutions for free-field motions in a continuously inhomogeneous half-plane that include contributions of incident P/SV waves, as well as of waves reflected from the traction-free horizontal surface. Material inhomogeneity is in the form of a shear modulus profile that varies quadratically with the depth coordinate. Also, Poisson's ratio is fixed at one-quarter, while both shear modulus and material density profiles vary proportionally. A series of numerical results serve to validate the aforementioned model, and to show the differences in the wave motion patterns developing in media that are inhomogeneous as compared to a reference homogeneous background. This type of information is useful within the context of engineering fields as diverse as laminated composites, geophysical prospecting, oil exploration and earthquake engineering.

Keywords: Incident waves, reflected waves, inhomogeneous media, wave motion

INTRODUCTION

Computation of free field motions in the semi-infinite homogeneous space constitutes one of the early chapters of elastodynamics (Achenbach, 1973). It is also one of the most important ones, because any structure placed on or in the half-space is clearly influenced by these motions. Free field motions in layered media, which model the simplest type of inhomogeneity, have been computed in the past by many researchers who imposed continuity conditions between the constant-thickness sub-layers [Kausel and Manolis, 2000]. Variable velocity layers are discussed in (Ewing et al., 1957), where the basic problem of inseparability of waves into dilatational and rotational components is brought forth. Wave reflection and refraction of elastic, acoustic and electromagnetic waves in discrete as well as in continuously layered media require specialized methods of solution, such as variational techniques, mode matching, Green's functions, integral equations and the T-matrix approach (Chew, 1990).

Wave motion in geological media presents certain peculiarities that have to do with the inherent difficulty of providing an accurate description of the underlying soil and rock formations. As a result, many specialized methods for analyzing seismically-induced ground motions have been devised, classified as analytical, numerical and hybrid (Helbig, 1994). Furthermore, free-field motions in the inhomogeneous half-space are important for evaluating site effects that account for laterally varying geometry, which is known to cause additional amplifications to the standard uni-dimensional model response (Alvarez-Rubio et al., 2004). The role of lateral heterogeneity, especially in the context of small and shallow sedimentary basins, has been recently observed in a number of references (Semblatt et al., 2005).

[1] Professor, Dept. of Civil Eng., Aristotle University, Thessaloniki, Greece; Email: gdm@civil.auth.gr
[2] Professor, Institute of Mathematics & Informatics, Bulgarian Academy of Sciences, Sofia, Bulgaria
[3] Assoc. Professor, Institute of Mechanics, Bulgarian Academy of Sciences, Sofia, Bulgaria
[4] PhD student, Dept. of Civil Eng., Aristotle University, Thessaloniki, Greece

In this work, we examine incident and reflected waves in a special category of 2D inhomogeneous continua that exhibiting quadratic variation of the Lamé parameters with respect to the depth coordinate. More complete results can be found in (Manolis et al., 2006), where the exponential-type of variation is also examined. The key step in what is essentially an eigenvalue extraction approach is to diagonalize the dynamic equilibrium operator, which itself derives from a set of algebraically transformed equations of motion with desirable mathematical properties stemming from the fact that their form resembles that of an equivalent homogeneous medium. A restricted class of inhomogeneous media, namely one where the elastic parameters and the density all vary proportionally with depth, must be assumed if this type of transformation is to be valid. Situations where this has actually been observed include the geological profile of the Sofia region in Bulgaria (Bonchev et al., 1982) that was measured from in-situ data. This profile seems to imply both a proportional variation of the shear modulus and of the density, plus a constant Poisson's ratio value of one-quarter, for a nearly thirty kilometer thickness of the local deposits as measured from the surface.

PROBLEM STATEMENT

We consider an isotropic, linearly elastic continuum with position-dependent material properties. As shown in Fig. 1, a Cartesian coordinate system Ox_1x_2 is employed, and the Lamé constants are now functions of depth ($\lambda = \lambda\left(\underline{x}\right) = \lambda\left(x_2\right)$, $\mu = \mu\left(\underline{x}\right) = \mu\left(x_2\right)$), as is the material density $\rho = \rho\left(\underline{x}\right) = \rho\left(x_2\right)$, where $\underline{x} = (x_1, x_2)$. Furthermore, time-harmonic incident waves of either the P the SV type propagate with frequency ω through the solid by tracing an incident angle θ with respect to the vertical axis.

Material Properties

It is assumed here that Poisson's ratio is fixed as $\nu = 0.25$, which implies that $\mu(\underline{x}) = \lambda(\underline{x}) = h(\underline{x})\mu_0$. For a quadratic (Q) inhomogeneity, the material function is $h(x_2) = (ax_2 + 1)^2$, while the density profile is proportional to the material profile, i.e., $\rho(x_2) = \rho_0 h(x_2)$. Both parameters $\mu_0 > 0$, $\rho_0 > 0$ represent values of their respective profiles at the reference plane (taken here as the horizontal traction-free surface of the half-plane), and $a < 0$ is a constant. Obviously, if $a = 0$, both material profiles collapse to the equivalent homogeneous case.

Governing Vector wave equation

The governing equations of motion in the absence of body forces are

$$\sigma_{ij,j}\left(\underline{x},\omega\right) + \rho\left(\underline{x}\right)\omega^2 u_i\left(\underline{x},\omega\right) = 0 \tag{1}$$

In the above, $\sigma_{ij,j}\left(\underline{x},\omega\right) = \left\{\lambda\left(\underline{x}\right)u_{k,k}\left(\underline{x},\omega\right)\right\}_{,i} + \left\{\mu\left(\underline{x}\right)\left(u_{i,j}\left(\underline{x},\omega\right) + u_{j,i}\left(\underline{x},\omega\right)\right)\right\}_{,j}$ is the equilibrium operator with σ_{ij} the stress tensor and u_i the displacement field. Also, commas indicate spatial derivatives, while vectorial quantities are denoted through the use of indices ($i, j = 1,2$) or by underlying. Finally, the second part of Eqs (1) comprises inertial forces.

Eqs (1) form an elliptic system of partial differential equations, which in the Q-type of inhomogeneity are defined in subspace $\left\{\underline{x} : x_2 < -1/a\right\}$ since they degenerate along the line $x_2 = -1/a$. Next, a functional transformation for the displacement vector is proposed as

$$u_i(\underline{x},\omega) = h^{-1/2}(\underline{x})U_i(\underline{x},\omega) \tag{2}$$

where $U_i(\underline{x},\omega)$ is now a solution for the dynamic equilibrium equations expressed in terms of the equivalent homogenous medium case:

$$\Sigma_{ij,j} + \gamma_i U_i = 0 \tag{3}$$

In the above, parameters $\gamma_1 = \gamma_2 = \rho_0\omega^2$ for the Q-inhomogeneity and $\gamma_1 = \rho_0\omega^2 - \mu_0 a^2$, $\gamma_2 = \rho_0\omega^2 - 3\mu_0 a^2$ for the E-inhomogeneity. Furthermore, the corresponding equilibrium operator is $\Sigma_{ij,j} = \mu_0 U_{i,jj} + 2\mu_0 U_{j,ij}$. At this point, inhomogeneity has been reduced to solutions of an equivalent homogeneous case, subjected to appropriate boundary conditions.

Boundary Conditions

We specify traction-free boundary conditions along the surface:

$$t_j\big|_{x_2=0} = \sigma_{ij} n_i = 0 \tag{4}$$

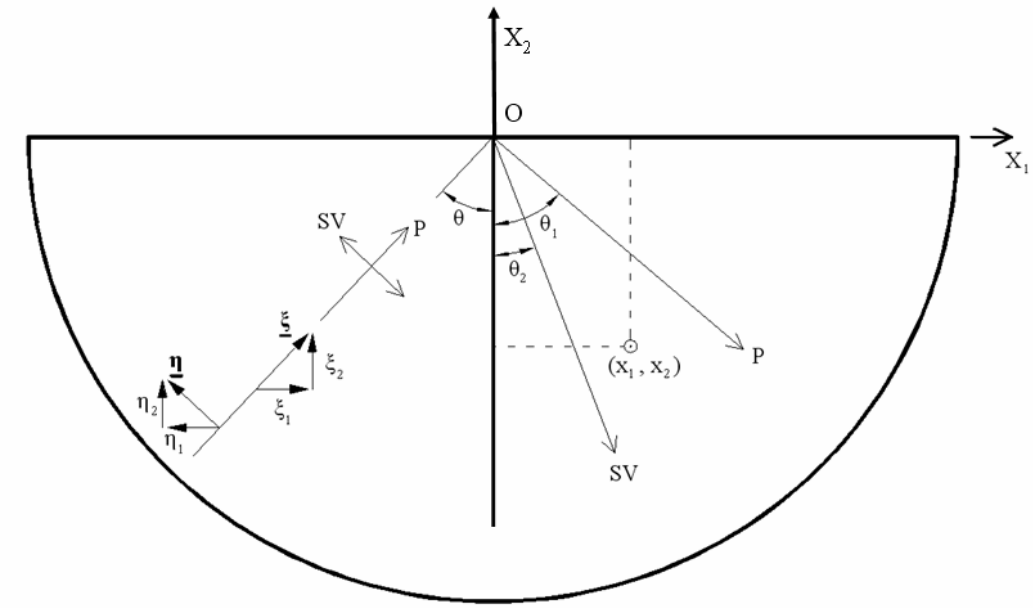

Figure 1. P/SV wave propagation through the inhomogeneous half-plane

More specifically, the above tractions are given as

$$\begin{aligned} t_j(\underline{x},\omega) &= C_{ijkl}(\underline{x}) n_i(\underline{x}) (h^{-1/2}(\underline{x}) U_k(\underline{x},\omega))_{,l} = \\ &= h(\underline{x}) C^0_{ijkl} n_i(\underline{x}) \left[-\frac{1}{2} h^{-3/2}(\underline{x}) h_{,l}(\underline{x}) U_k(\underline{x},\omega) + h^{-1/2}(\underline{x}) U_{k,l}(\underline{x},\omega) \right] \end{aligned} \tag{5}$$

and $C_{ijkm} = h(\underline{x}) C^0_{ijkm}$, with $C^0_{ijkm} = \mu_0 \left(\delta_{ij}\delta_{km} + \delta_{ik}\delta_{jm} + \delta_{im}\delta_{jk} \right)$ being the elasticity tensor for a homogeneous isotropic continuum. The radiation condition at infinity also holds true.

THE INHOMOGENOUS PLANE

Starting with a fixed value of frequency ω and a propagation vector $\underline{\xi} = (\xi_1 = \sin\theta, \xi_2 = \cos\theta)$ (where $|\underline{\xi}| = 1$, $\theta \in (0, \pi/2)$) for the incoming wave (see Fig. 1), we find solutions to Eq (3) as

$$U_j^m = p_j^m \exp\{ik_m(x_1\xi_1 + x_2\xi_2)\} \tag{6}$$

where index $m = S, P$ indicates the type of wave (shear or pressure). In the above, $\underline{x} = (x_1, x_2)$ are the coordinates of the receiver, k_m are wave numbers and $\underline{p}^m$ are polarization (or direction) vectors. Note at the same time, the $(k_m^2, \underline{p}^m)$ pair represents the eigenvalues and eigenvectors of the following linear system of equations:

$$\left[-M(\xi)k_m^2 + \Gamma\right]\underline{p}^m = 0 \tag{7}$$

In order to find solutions of Eq (7) for every particular case, we have to transform matrices $M(\xi)$, Γ into diagonal form. That this operation is possible stems from the fact that matrix $M(\xi)$ is positive-definite. Thus, there exists a transformation matrix T such that

$$T^{-1}\left(-M(\xi)k_m^2 + \Gamma\right)T = -k_m^2 I_2 + \Lambda(\xi) \tag{8}$$

where $\Lambda(\xi) = \begin{pmatrix} \gamma_1(\xi) & 0 \\ 0 & \gamma_2(\xi) \end{pmatrix}$, I_2 is the 2×2 identity matrix and, as a result, $k_m^2 = \gamma_m(\xi)$.

For the Q-inhomogeneity, Eq (7) becomes

$$\left(-\mu_0\begin{pmatrix} 2\xi_1^2+1 & 2\xi_1\xi_2 \\ 2\xi_1\xi_2 & 2\xi_2^2+1 \end{pmatrix}k_m^2 + \begin{pmatrix} \rho_0\omega^2 & 0 \\ 0 & \rho_0\omega^2 \end{pmatrix}\right)\underline{p}^m = 0 \tag{9}$$

The roots of $\det\left[-M(\xi)k^2 + \Gamma\right] = 0$ are computed as $k_S^2 = \rho_0\omega^2/\mu_0$, $k_P^2 = \rho_0\omega^2/3\mu_0$, while the corresponding normalized eigenvectors are $\underline{p}^S = \underline{q} = \begin{pmatrix} -\xi_2 \\ \xi_1 \end{pmatrix}$, $\underline{p}^P = \underline{p} = \begin{pmatrix} \xi_1 \\ \xi_2 \end{pmatrix}$. Note that $\underline{q} \perp \underline{p}$. We recover two types of solutions, an SV wave and a P wave, as

$$\underline{U}^S = A_0\begin{pmatrix} -\xi_2 \\ \xi_1 \end{pmatrix} e^{ik_S(x_1\xi_1 + x_2\xi_2)}, \underline{U}^P = A_0\begin{pmatrix} \xi_1 \\ \xi_2 \end{pmatrix} e^{ik_P(x_1\xi_1 + x_2\xi_2)} \tag{10}$$

where A_0 is the wave amplitude. In either case, the displacement vector in the original domain is computed by using Eq (2) as follows:

$$u_j^m = (1/(ax_2 + 1))\, U_j^m \tag{11}$$

THE INHOMOGENEOUS HALF-PLANE

In deriving the inhomogeneous half-plane solutions, we follow (Achenbach, 1973) approach for the homogenous isotropic case.

Incident P Wave

The incident P, the reflected P and the reflected SV waves in the transformed domain are as follows:

$$\begin{aligned}
\underline{U}^{in,P} &= \begin{pmatrix} U_1^{in,P} \\ U_2^{in,P} \end{pmatrix} = A_0 \begin{pmatrix} \xi_1 \\ \xi_2 \end{pmatrix} \; e^{ik_P(x_1\xi_1 + x_2\xi_2)}, \underline{U}^{re,P} = \begin{pmatrix} U_1^{re,P} \\ U_2^{re,P} \end{pmatrix} = A_1 \begin{pmatrix} \xi_1 \\ -\xi_2 \end{pmatrix} \; e^{ik_P(x_1\xi_1 - x_2\xi_2)}, \\
\underline{U}^{re,S} &= \begin{pmatrix} U_1^{re,S} \\ U_2^{re,S} \end{pmatrix} = A_2 \begin{pmatrix} \eta_2 \\ \eta_1 \end{pmatrix} \; e^{ik_S(x_1\eta_1 - x_2\eta_2)}
\end{aligned} \tag{12}$$

The tractions specified in Eq (5) are derived by differentiating the above displacement fields and the material function $h(\underline{x}) = (ax_2 + 1)^2$ with respect to the spatial coordinates. Thus,

$$\begin{aligned}
t_1^n &= h^{1/2}\mu_0 \left(-\frac{1}{2} h^{-1} h_{,2} U_1^n + U_{1,2}^n + U_{2,1}^n \right) \\
t_2^n &= h^{1/2}\mu_0 \left(-\frac{3}{2} h^{-1} h_{,2} U_2^n + U_{1,1}^n + 3U_{2,2}^n \right)
\end{aligned} \tag{13}$$

where superscript n stands for three combinations of incident/reflected and P/SV waves: $(in,P);\ (re,P);(re,S)$. Next, the boundary condition of Eq (4) implies that

$$t_j^{in,P} + t_j^{re,P} + t_j^{re,S}\Big|_{x_2=0} = 0 \tag{14}$$

Since $j = 1,2$, we have two equations to compute component η_1 of the reflected propagation vector and amplitudes (A_1, A_2) for a given (ξ_1, A_0). First, in order to reduce the exponential multiplier in Eqs (12), η_1 is specified such that $k_P\xi_1 = k_S\eta_1$. Given incident angle θ, $\xi_1 = \sin\theta$ and by denoting $\eta_1 = \sin\theta_2$, we recover a reflection angle $\theta_2 = \arcsin(\kappa \sin\theta)$, where $\kappa = k_P / k_S$. Since $\kappa < 1$, the reflected angle range is $0 < \theta_2 < \pi/2$, while the second component of the reflected propagation vector is computed as $\eta_2 = \cos\theta_2 > 0$.

Next, Eq (14) yields the following 2×2 system of equations:

$$\begin{pmatrix} d_{11} & d_{12} \\ d_{21} & d_{22} \end{pmatrix} \begin{pmatrix} \alpha_1 \\ \alpha_2 \end{pmatrix} = \begin{pmatrix} \beta_1 \\ \beta_2 \end{pmatrix} \tag{15}$$

The unknowns here are the reflected amplitude ratios $\alpha_s = A_s / A_0$ $(s = 1,2)$, while the matrix coefficients and the right-hand side vector components are given below as

$$
\begin{aligned}
&d_{11} = -a\xi_1 - ik_P 2\xi_1\xi_2 \qquad d_{12} = -a\eta_2 - ik_S(\eta_2^2 - \eta_1^2)\\
&d_{21} = 3a\xi_2 + ik_P(1+2\xi_2^2) \quad d_{22} = -3a\eta_1 - ik_S 2\eta_1\eta_2\\
&\beta_1 = a\xi_1 - ik_P 2\xi_1\xi_2 \qquad \beta_2 = 3a\xi_2 - ik_P(1+2\xi_2^2)
\end{aligned}
\tag{16}
$$

A unique solution to Eq (16) exists if (and only if) the determinant $d(a) = d_{11}d_{22} - d_{12}d_{21}$ of the coefficient matrix is non-zero, as discussed in (Manolis et al., 2006). In sum, this solution is $\alpha_1 = d_1 / d$, $\alpha_2 = d_2 / d$ (with $d_1 = \beta_1 d_{22} - \beta_2 d_{12}$ and $d_2 = \beta_2 d_{11} - \beta_1 d_{21}$), so that the reflected wave amplitudes are $A_1 = \alpha_1 A_0$, $A_2 = \alpha_2 A_0$. The total displacements in the physical domain are

$$
u_j = (1/(ax_2+1))\left(U_j^{in,P} + U_j^{re,P} + U_j^{re,S}\right) \tag{17}
$$

Incident SV Wave

The incident SV and the reflected SV and P waves in the transformed domain are as follows:

$$
\begin{aligned}
&\underline{U}^{in,S} = \begin{pmatrix} U_1^{in,S} \\ U_2^{in,S} \end{pmatrix} = B_0 \begin{pmatrix} -\eta_2 \\ \eta_1 \end{pmatrix} e^{ik_S(x_1\eta_1 + x_2\eta_2)}, \underline{U}^{re,S} = \begin{pmatrix} U_1^{re,S} \\ U_2^{re,S} \end{pmatrix} = B_1 \begin{pmatrix} \eta_2 \\ \eta_1 \end{pmatrix} e^{ik_S(x_1\eta_1 - x_2\eta_2)},\\
&\underline{U}^{re,P} = \begin{pmatrix} U_1^{re,P} \\ U_2^{re,P} \end{pmatrix} = B_2 \begin{pmatrix} \xi_1 \\ -\xi_2 \end{pmatrix} e^{ik_P(x_1\xi_1 - x_2\xi_2)}
\end{aligned}
\tag{18}
$$

where the SV wave polarization vector components are $(\eta_1 = \sin\theta, \eta_2 = \cos\theta)$.

The tractions specified in Eq (5) are again derived by differentiating the above displacement fields and the material function $h(\underline{x}) = (ax_2+1)^2$ with respect to the spatial coordinates. Thus, we obtain

$$
\begin{aligned}
t_1^n &= h^{1/2}\mu_0\left(-\frac{1}{2}h^{-1}h_{,2}U_1^n + U_{1,2}^n + U_{2,1}^n\right)\\
t_2^n &= h^{1/2}\mu_0\left(-\frac{3}{2}h^{-1}h_{,2}U_2^n + U_{1,1}^n + 3U_{2,2}^n\right)
\end{aligned}
\tag{19}
$$

where superscript n stands for: (in,S); (re,S); (re,P). Next, the boundary conditions (4) specify that

$$
t_j^{in,S} + t_j^{re,S} + t_j^{re,P}\Big|_{x_2=0} = 0 \tag{20}
$$

Again, we have two equations to compute component ξ_1 and amplitudes (B_1, B_2) for given (η_1, B_0). First, in order to reduce the exponential multiplier in Eq (18), ξ_1 is specified through relation $k_P\xi_1 = k_S\eta_1$. By denoting $\xi_1 = \sin\theta_1$, we recover the reflection angle as $\theta_1 = \arcsin\left(\sin\theta/\kappa\right)$, where $\kappa = k_P / k_S = \sqrt{3}$. Since $\xi_1 = \sqrt{3}\eta_1 < 1$, ξ_1 values exist if (and only if) $\eta_1 < 1/\sqrt{3}$, i.e., $\theta < \theta_{cr} = \arcsin\left(1/\sqrt{3}\right) = 35^o16'$. Thus, the reflected angle range is $0 < \theta_1 < \theta_{cr}$ and $\xi_2 = \cos\theta_1 > 0$.

Next, Eq (26) yields a 2×2 system of equations as in (15). This time, the unknowns are the amplitude ratios $\alpha_s = B_s / B_0$ ($s = 1, 2$), while the system coefficients are given below as

$$\begin{aligned} d_{11} &= -a\eta_2 + ik_S 2(\eta_1^2 - \eta_2^2) \quad d_{12} = -a\xi_1 - 2ik_P \xi_1 \xi_2 \\ d_{21} &= -3a\eta_1 - 2ik_S \eta_1 \eta_2 \qquad d_{22} = 3a\xi_2 + ik_P(\xi_1^2 + 3\xi_2^2) \\ \beta_1 &= -a\eta_2 + ik_S(\eta_2^2 - \eta_1^2) \qquad \beta_2 = 3a\eta_1 - 2ik_S \eta_1 \eta_2 \end{aligned} \tag{21}$$

As before, solution the above system (see the previous section and the Appendix) yields ratios α_1, α_2 so that the reflected wave amplitudes are $B_1 = \alpha_1 B_0$, $B_2 = \alpha_2 B_0$. The total displacements are

$$u_j = (1/(ax_2 + 1))\left(U_j^{in,S} + U_j^{re,S} + U_j^{re,P}\right) \tag{22}$$

NUMERICAL RESULTS

In this section, numerical results are given for wave propagation cases concerning the half-plane. First, we define a homogenous material background with the following properties:

$$\begin{aligned} &\lambda_0 = \mu_0 = 180\times 10^6 \ Pa; \quad \rho_0 = 2000 \ kg/m^3 \\ &\nu = 0.25; \quad c_P = 519 \ m/\sec, \quad c_S = 300 \ m/\sec \end{aligned} \tag{23}$$

In the above, c_P, c_S respectively are the reference P and SV wave speeds. Next, we specify a frequency range of $1.50\, rad/\sec < \omega < 6.28\, rad/\sec$ (or $0.25\, Hz < f < 1.00\, Hz$) for the incoming waves, which is considered representative of seismic motions with low-frequency content. As far the wave numbers are concerned, we have that $k_S = 0.0209(1/m), \quad k_P = 0.0121(1/m)$ at $f = 1.0\, Hz$ and the corresponding wave lengths are $l_S = 2\pi / k_S = 300\, m, \quad l_P = 2\pi / k_P = 519\, m$.

The incident wave angle spans the range $0 < \theta < \pi/2$ in forty increments, and the receiver point is located in the lower right quadrant of the half-plane at $\underline{x} = (x_1, x_2) = (R\sin\theta, -R\cos\theta), R = 100.0\, m$ (Fig. 1). Finally, the inhomogeneity parameter ranges as $0.0 \le |a| < 0.01$. In order to give a sense of magnitude to the resulting material parameters, a value of $a = -0.001$ yields $h(x_2 = -100) = 1.21$, which implies a 20% or so increase in the shear modulus starting from the free surface and moving downwards. At what would be an upper bound $a = -0.01$, we have $h(-100) = 4.00$. Also, the restriction $\omega > c_P |a|$ is satisfied for the above range of parameters.

The results, summarized in Figs. 2-3, plot displacement vector $\underline{u}$ versus incident wave angle θ of incoming P and SV waves in the Q-inhomogeneous half-plane, respectively. Given that $\underline{u}$ is a complex quantity, one plot is for the amplitude ($|u_i|$, in mm) and one for the phase angle ($\measuredangle u_i$, in rad) for each displacement component (horizontal and vertical), all corresponding to a unit amplitude of the incoming wave. In order to show results that are representative for the problem under study, we retain the lower and upper values of the frequency spectrum, plus two values of the inhomogeneity parameter $(a = -0.001; a = -0.0015)$.

In the interest of brevity, and since the response can readily be predicted, the incident P and SV waves in the Q-inhomogeneous plane have not been plotted. Summarizing, it is only the amplitude of motion that is sensitive to the inhomogeneous profile. Specifically, any increase in the value of $|a|$ yields a nearly proportional increase in the magnitude of both displacement components, up to a maximum of about 20%. This is a consequence of the fact that the incoming wave is moving upwards against a profile that is continuously weakening. Of course, as the incident angle θ approaches 90^0, the wave cuts across the material profile and no difference is observed in the presence of inhomogeneity.

The picture becomes quite complex when reflected waves due to the presence of the horizontal traction-free surface are added to the incident wave. Starting with the P-P-SV case of Fig. 2 we see a drop in the amplitude of both displacement components (u_1, u_2) with increasing value of $|a|$, since we now have two reflected waves moving downwards along a profile that is stiffening with depth. This increase is somewhat less smooth than what was observed with incoming waves only, and the maximum drop in magnitude does not exceed 25%. More interesting, the phase angle plots become more complicated than the simple sinusoidal shapes observed in the full-plane case. Also, invariably larger phase angle values are recorded in the presence of inhomogeneity, indicating an imaginary component of motion that is becoming more dominant in reference to the real component. Next, Fig. 3 addresses the SV-SV-P case, where the previously computed cut-off incident angle of $\theta_{cr} = 35^o16'$ applies to both homogeneous and inhomogeneous media. It should be noted that for $\theta > \theta_{cr}$, one must search for surface waves. As far as the displacement amplitudes are concerned, we have a non-smooth overshoot in the inhomogeneous medium (for the same reason mentioned before) to values that may now exceed 150% in the low frequency range. For the higher frequency value, this overshoot is similar to what was previously observed (i.e., in the neighborhood of 25%). On the other hand, the phase angles in the inhomogeneous medium lag what was recorded in the homogeneous medium for the case of vertical motions; the opposite holds true for horizontal motions.

CONCLUSIONS

Free-field motions in the continuously inhomogeneous half-plane, which consist of incident plus reflected wave contributions, show marked differences with respect to the benchmark homogeneous case. Specifically, as an incoming wave propagates upwards, the material stiffness changes continuously and in proportion to the material density, thus causing a scattering of the original signal. The presence of a horizontal traction-free surface further reinforces this effect, since it is responsible for the emergence of reflected waves moving downwards. It should be noted that the usual conversion from incident P to reflected P and SV waves still takes place for this relatively mild type of inhomogeneity. However, the frequency of motion plays an important role, for there are frequency bands where the P and SV wave numbers become imaginary, which in turn indicates localized wave conversion phenomena, standing waves and other complications.

ACKNOWLEDGEMENTS

The authors wish to acknowledge financial support from the ‘Greek-Bulgarian Joint Research and Technology Program 2004-06’, Project No. BG/GR-11/2005Y.

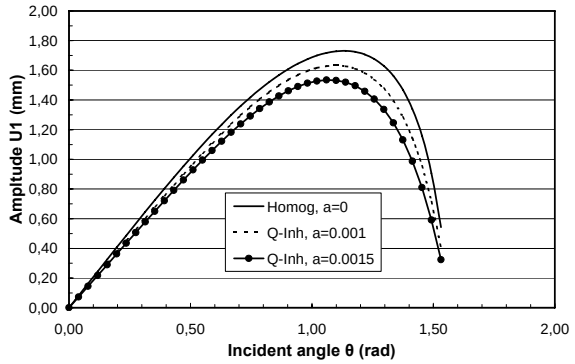

(a)

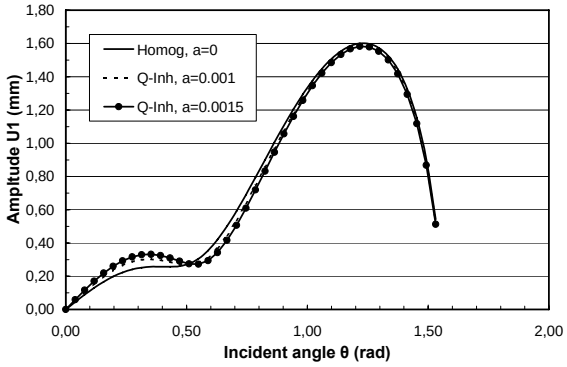

(e)

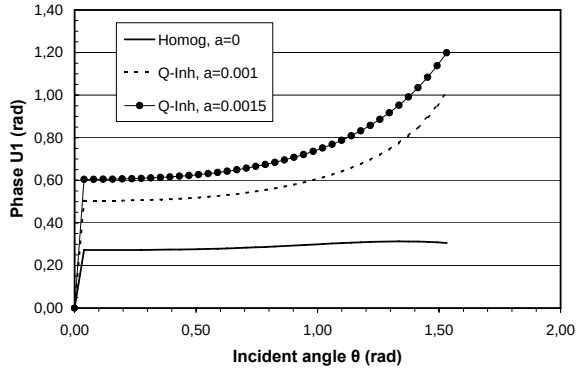

(b)

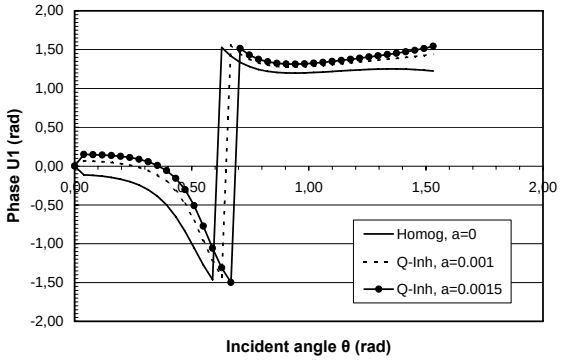

(f)

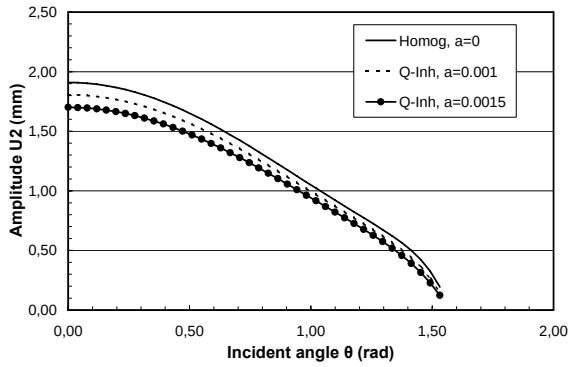

(c)

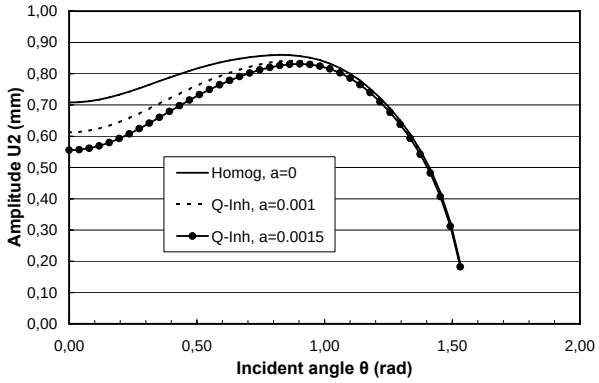

(g)

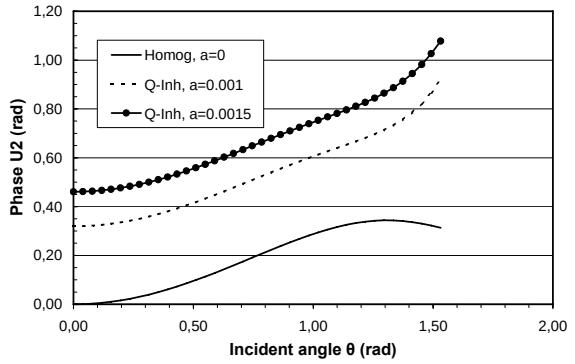

(d)

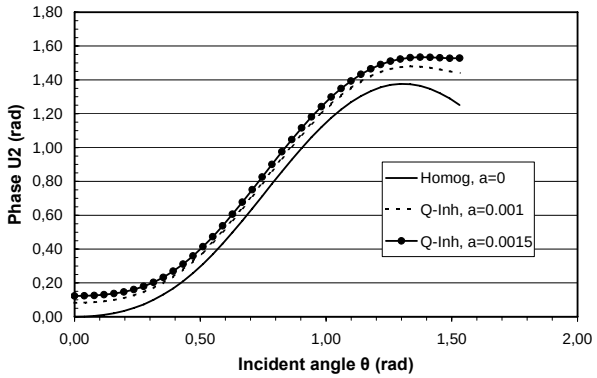

(h)

Figure 2. Incident P and reflected P, SV waves in the Q-inhomogeneous half-plane: (a) $|u_1|$; (b) $\measuredangle u_1$; (c) $|u_2|$; (d) $\measuredangle u_2$ vs. θ at $f = 0.25Hz$ and (e) $|u_1|$; (f) $\measuredangle u_1$; (g) $|u_2|$; (h) $\measuredangle u_2$ vs. θ at $f = 1.0Hz$

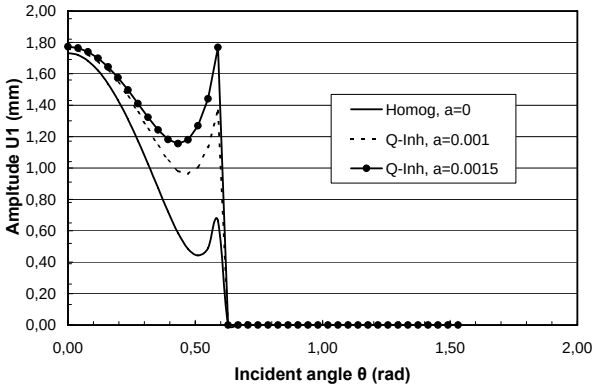

(a)

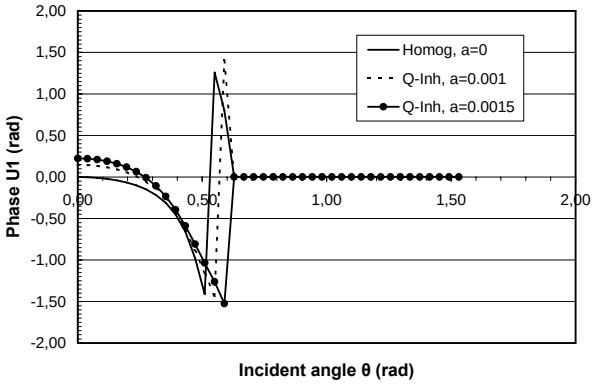

(b)

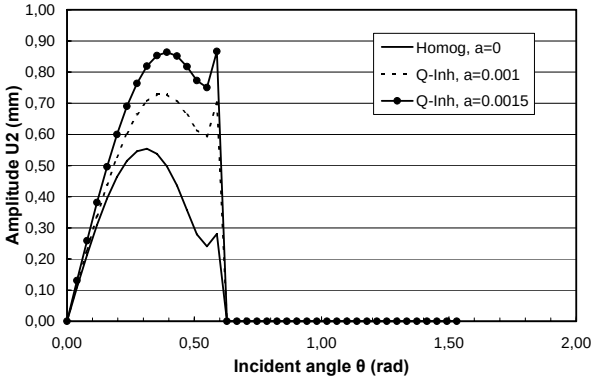

(c)

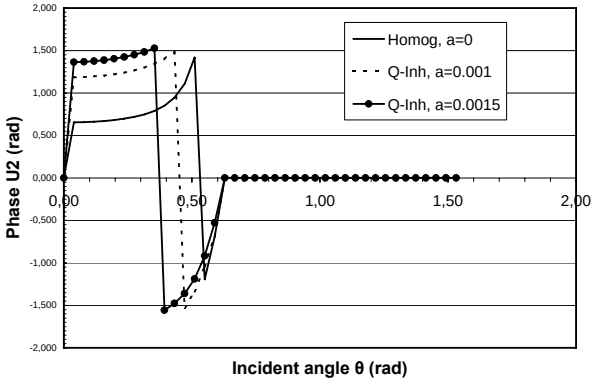

(d)

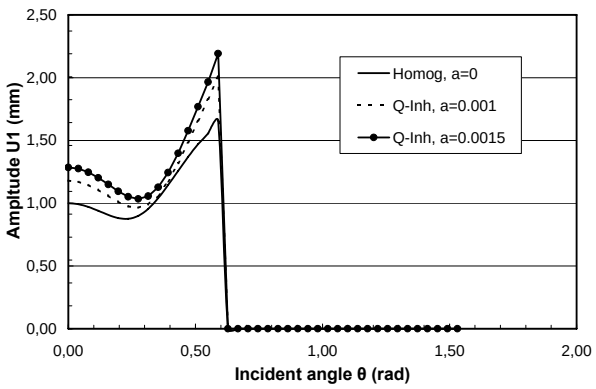

(e)

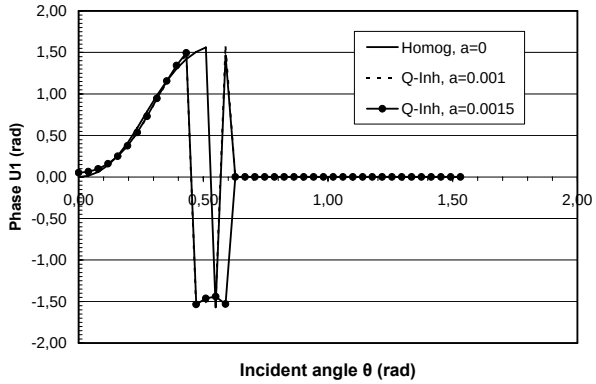

(f)

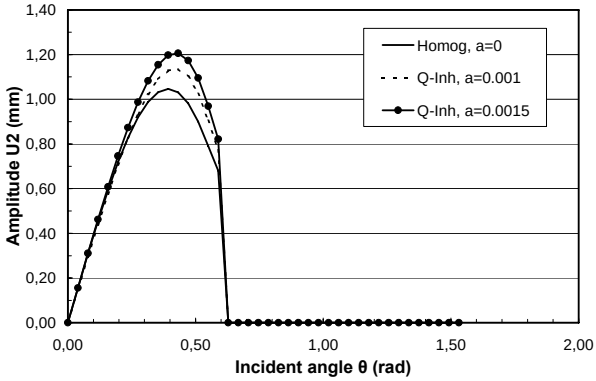

(g)

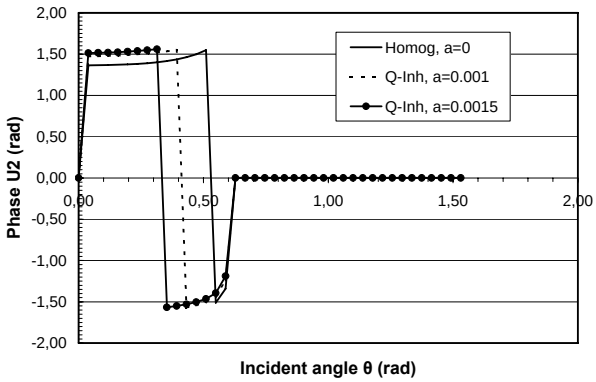

(h)

Figure 3. Incident SV and reflected SV, P waves in the Q-inhomogeneous half-plane: (a) $|u_1|$; (b) $\measuredangle u_1$; (c) $|u_2|$; (d) $\measuredangle u_2$ vs. θ at $f = 0.25Hz$ and (e) $|u_1|$; (f) $\measuredangle u_1$; (g) $|u_2|$; (h) $\measuredangle u_2$ vs. θ at $f = 1.0Hz$

REFERENCES

Achenbach JD. Wave Propagation in Elastic Solids, North Holland, Amsterdam, 1973.

Kausel E and Manolis GD (eds). Wave Motion Problems in Earthquake Engineering, WIT Press, Southampton, 2000.

Ewing WM, Jardetzky WS and Press F. Elastic Waves in Layered Media, McGraw-Hill, New York, 1957.

Chew WC. Waves and Fields in Inhomogeneous Media, Van Nostrand-Rheinhold, New York, 1990.

Helbig K (ed). Modelling the Earth for Oil Exploration, Pergamon/Elsevier Science, Oxford, 1994.

Alvarez-Rubio S, Sanchez-Sesma FJ, Benito JJ and Alarcon E. "The direct boundary element method: 2D site effects assessment on laterally varying layered media (methodology)," Soil Dynamics and Earthquake Engineering, 24, 167-180, 2004.

Semblat JF, Kham M, Bard PY, Pitilakis K, Makra K and Raptakis D. "Seismic wave amplification: basin geometry versus soil layering," Soil Dynamics and Earthquake Engineering, 25, 529-538, 2005.

Manolis GD, Rangelov TV and Dineva PS. "Free-field Wave solutions in a half-plane exhibiting a special-type of continuous inhomogeneity," Wave Motion, to appear, 2006.

Bonchev E, Bune V, Christoskov L, Karagyuleva J, Kostadinov V, Reisner G, Rizikova S, Shebalin N, Sholpo V and Sokerova D. "A method for compilation of seismic zoning prognostic maps for the territory of Bulgaria," Geologica Balkanica, 12(2), 3-48, 1982.